Biocompatibility of Kaffir Lime Fruit Juice Powered ZnO Nanoparticles in Earthworm, *Eudrilus eugeniae*: A Green Biomimetic Approach

Sampath Paventhan,[a] Pazhanisamy Kavitha,[a,*] Balasubramanian Kaleeswaran,[a] Muniappan Ayyanar,[b] Vengamuthu Subramanian Kavitha,[c] Singamoorthy Amalraj,[d] Raman Sripriya,[a] R. Rajakrishnan,[e] and Ahmed H. Alfarhan [e]

**Corresponding author: rameshkavi.dharaka@gmail.com*

DOI:10.15376/biores.20.1.1345-1364

GRAPHICAL ABSTRACT

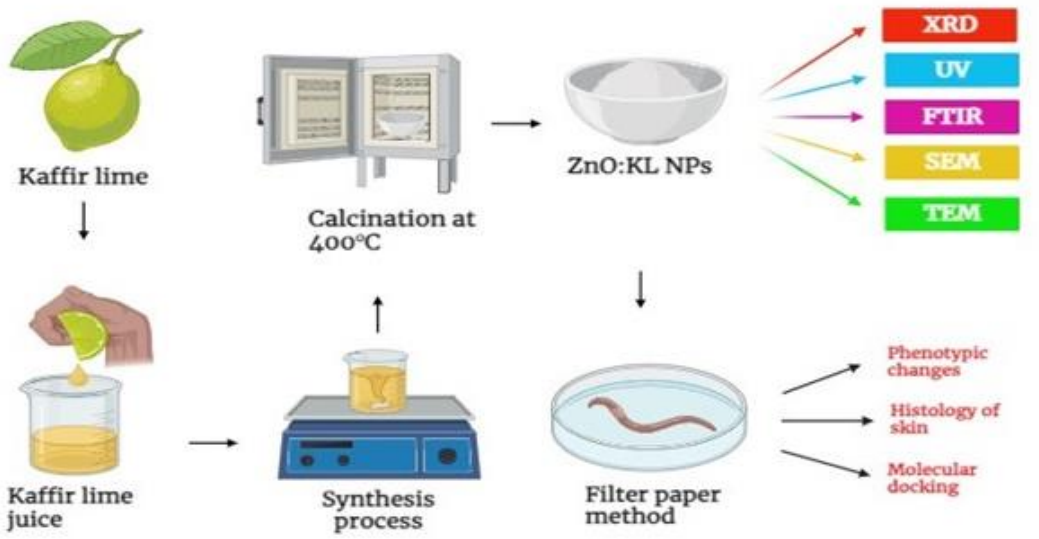

Biocompatibility of Kaffir Lime Fruit Juice Powered ZnO Nanoparticles in Earthworm, *Eudrilus eugeniae*: A Green Biomimetic Approach

Sampath Paventhan,[a] Pazhanisamy Kavitha,[a,*] Balasubramanian Kaleeswaran,[a] Muniappan Ayyanar,[b] Vengamuthu Subramanian Kavitha,[c] Singamoorthy Amalraj,[d] Raman Sripriya,[a] R. Rajakrishnan,[e] and Ahmed H. Alfarhan [e]

ZnO nanoparticles were synthesized using the raw juice of Kaffir lime (*Citrus hystrix*) fruit bya simple and cost-effective green route and its effects on earthworms, *Eudrilus eugeniae*, were studied. The kaffir-lime powered ZnO nanoparticles (ZnO:KL) were characterized by X-ray diffraction (XRD), UV-Vis-NIR spectroscopy, Fourier-transform infrared spectroscopy (FT-IR), scanning electron microscopy (SEM), and transmission electron microscopy (TEM). The filter paper method was adopted to test the toxicity of ZnO:KL. Earthworms (species *Eudrilus eugeniae*) were exposed to 100 to 1000 mg/L of ZnO:KL in one-step order. During the study period (up to 48 h), no mortality was found in any treatment group. In histological observation, no damage was found in the epidermal layer of earthworm's skin treated up to 800 mg/L, whereas slight epidermal damage was observed only in 900 and 1000 mg/L treated earthworms. The GC-MS spectrum of the juice of kaffir lime fruit revealed 22 bioactive compounds. The predominantly identified bioactive compounds vitamin C and citric acid were subjected to molecular docking to reveal their binding affinity with collagen – a structural protein providing strength and flexibility of the earthworm's body. Vitamin C and citric acid bind to the collagen in a favorable orientation with the binding affinity of -4.44 kcal/mol and -4.97 kcal/mol, respectively. Since vitamin C and citric acid are capable of influencing the biosynthesis of collagen, they could prevent skin damage. In sum, the kaffir lime-powered ZnO nanomaterial is less toxic to the earthworm when compared with bare ZnO.

DOI: 10.15376/biores.20.1.1345-1364

Keywords: Vitamin C; Molecular docking; Eudrilus eugeniae; Kaffir lime fruit; ZnO nanoparticles

*Contact information: a: PG & Research Department of Zoology and Biotechnology, A.V.V.M Sri Pushpam College (Autonomous), (Affiliated to Bharathidasan University), Poondi, Thanjavur, Tamil Nadu 613503, India; b: PG& Research Department of Botany, A.V.V.M Sri Pushpam College(Autonomous), (Affiliated to Bharathidasan University), Poondi, Thanjavur, Tamil Nadu 613503, India; c: Department of Zoology, Vellalar College for Women, Thindal, Erode, Tamil Nadu 638012, India; d: Division of Phytochemistry and Drug Design, Department of Biosciences, Raja giri College of Social Sciences (Autonomous), Kalamaserry, Kochi 683104, Kerala, India; e: Department of Botany & Microbiology, College of Science, King Saud University, Riyadh, 11451, Saudi Arabia; *Corresponding author: rameshkavi.dharaka@gmail.com*

List of Abbreviations

KL juice - Kaffir Lime fruit juice
GC-MS - Gas Chromatography Mass Spectrometry
ZnO:KL NPs - Zinc Oxide:Kaffir Lime Nanoparticles
OECD – The Organization for Economic Cooperation and Development
E. eugeniae–Eudrilus eugeniae
ROS - Reactive Oxygen Species

INTRODUCTION

Among soil invertebrates, earthworms are fascinating creatures that play a crucial role in soil health, nutrient cycling, and organic matter decomposition. Over 80% of the biomass of terrestrial invertebrates is composed of earthworms. In recent years, earthworms have been under severe threats due to the abundant use of fertilizers and the improper disposal of wastes, especially nano-wastes into soil. Nanotechnology is a rapidly growing field that touches almost all areas due to its wide range of applications. The abundant usage of engineered nanomaterials undoubtedly increases the possibility of releasing into the soil and thereby causes detrimental effects on earthworms. Among the nanomaterials, ZnO nanomaterials have widely been used in the manufacturing of chemical products, electronics, cosmetics, and pharmaceutical products. Due to its increasing usage, huge amounts of ZnO nanomaterials enter the soil ecosystem and act as hazards to earthworms and other soil-dwelling organisms (Świątek *et al.* 2020). Researchers have paid much attention to determining the toxicity of ZnO nanomaterials to earthworms. Li *et al.* (2011) analyzed the toxicity of ZnO nanoparticles to earthworms *Eisenia fetida* and observed dose-related mortality. Fernanda *et al.* (2018) addressed the dose-related effects of ZnO and TiO_2 nanoparticles in the body weight change, survival, and reproduction of *Eisenia fetida*. They found that earthworms treated with lower doses did not show any survival damage but in higher doses, they showed significant damage (Valerio-Rodríguez *et al.* 2020). Li *et al.* (2019) reported that nano ZnO leads to excess reactive oxygen species (ROS) in earthworms and thereby causes oxidative damage. Filipiak and Bednarskathe (2021) examined the effects of ZnO nanoparticles on the earthworm *Eisenia andrei* in order to study the rate of mortality, growth, maturation, and cellular respiration.

Bio-route synthesis of ZnO nanomaterials using various parts of plants has drawn increasing attention due to its less toxic nature and wide range of applications. Plants possess biomolecules and metabolites including phenols, flavonoids, alkaloids, carbohydrates, proteins, vitamins, and coenzyme-based intermediates. The carboxyl, hydroxyl, and amine functional groups of plant metabolites help in the preparation of materials in the nanoscale range (1 to 100 nm). These plant molecules help not only in size reduction, but they also play a pivotal role in the capping of the nanoparticles which is important for biocompatibility (El-Sawaf *et al.* 2024). It has been reported that the biogenic reduction of metal precursors to corresponding nanoparticles is eco-friendly and free of chemical contamination (Daimari and Deka 2024). The synthesis of nanomaterials *via* the green route has gained a lot of attraction since it uses non-toxic phytochemicals and avoids the toxic solvents that would be used in chemical methods (Selvaraj *et al.* 2021). Based on these reports, it is understood that the green nanoparticles are safe to handle, less toxic, and eco-friendly.

Even though several researchers have reported the toxicity of chemically synthesized ZnO nanomaterials to earthworms, no studies have reported the effect of green-nano ZnO on earthworms so far. Hence, this study synthesizes ZnO nanomaterials *via* the green route using kaffir lime fruit juice to study its effect on the earthworm, *E. eugeniae*. The kaffir lime is a citrus fruit found in various parts of Asia. It is highly respected in herbal medicine. The organic constituents found in kaffir limes are anti-inflammatory and they stimulate the digestive system. Some of the acids found in this fruit help in the neutralization of free radicals and the dangerous byproducts of cellular respiration. As this fruit has ample biological significance, it has been chosen to synthesize plant-based ZnO nanomaterials in the present study.

This study reports a simple and cost-effective green method to synthesize ZnO nanomaterial using kaffir lime fruit juice (KL juice) and the effect of this plant-derived ZnO nanomaterial on the earthworm *E. eugeniae*. This research aims to increase the potential use of green-based ZnO nanomaterials in various applications.

EXPERIMENTAL

Preliminary Phytochemical Screening

The qualitative phytochemical pre-screening of KL juice followed the standard methodology (Harborne 1998).The presence and absence of various phytochemicals, *viz.*, alkaloids, phenols, flavonoids, terpenoids, quinones, tannins and steroids, were observed.

Screening of Alkaloids (Hager's test)

Initially, 50 mL of raw juice was taken. It was stirred well with a few mL of dilute hydrochloric acid, then filtered. To 1 mL of filtrate juice, 1 mL of Hager's reagent was added. A prominent yellow precipitate indicates the presence of alkaloids.

Screening of Phenols (Lead acetate test)

To1 mL of raw juice, 2 mL of distilled water, and 3 mL of a 10% lead acetate solution were added and mixed well. A bulky white precipitate indicates the presence of phenolic compounds.

Screening for Flavonoids (Alkaline reagent test)

1 mL of raw juice and 10% ammonium hydroxide solution were mixed well. Yellow fluorescence indicates the presence of flavonoids.

Screening of Terpenoids (Salkowski test)

5 mL of the raw juice was mixed with 2 mL of chloroform and 2 mL of concentrated sulfuric acid to form a layer. A reddish-brown coloration of the interface showed the presence of terpenoids.

Screening of Quinones (Borntrager's test)

3 mL of raw juice was treated with 3 mL of chloroform, and the chloroform layer was separated. Then 1 mL of 5% potassium hydroxide dissolution was added. The presence of quinines was indicated by a red colour in the alkaline phase.

Screening for Tannins

5 mL of raw juice was mixed with a few drops of 0.1% ferric chloride, brownish green or blue-black coloration, indicating the presence of tannins.

Screening of Steroids (Salkowski test)

2 mL of chloroform and 1 mL of concentrated sulfuric acid were added to 1 mL of raw juice dissolved in isopropyl alcohol, slowly until double phase formation. The presence of a dish brown colour in the middle layer was indicative of a steroidal ring.

Quantitative Analysis of Total Phenol

Total phenol was estimated using the Folin-Ciocalteu method (Amalraj *et al.* 2021). To 1 mL of KL juice sample, 0.5 mL of Folin-Ciocalteu reagent (1N) was added, and the

mixture was incubated at room temperature. Afterward, 2.5 mL of sodium carbonate (Na_2CO_3) was added and incubated at room temperature for 40 min. The absorbance was measured at 725 nm. The calculated total phenol content was expressed as gallic acid equivalent (mg GAE/mL) as gallic acid was used as standard.

Quantitative Analysis of Total Flavonoid

Using the aluminum chloride colorimetric method (Amalraj *et al*. 2021), the total flavonoid content was estimated. To 1 mL of KL juice, 2 mL of aluminum chloride ($AlCl_3$), and 6 mL of sodium acetate were added. The absorbance was measured at 430 nm. The estimated total flavonoid content was expressed as quercetin equivalent (mg QE/mL) as quercetin was used as standard.

GC-MS Analysis of Kaffir Lime Juice

First, 10 mL of raw KL juice was dissolved in 10 mL of ethanol. Using Whatman no.1 filter paper, the solution was filtered. The obtained clear extract was used for GC-MS analysis. GC-MS analysis of KL juice was carried out using a Shimadzu (QP2020) interfaced with a mass spectrometer. A capillary column of 30 m length, 0.25 mm inner diameter, and 0.25 µm film thickness (SH-Rxi-5Sil-MS non-polar) coated with 100% polydimethylsiloxane was used. The initial oven temperature was 50 °C and increased to 280 °C at a rate of 6 °C/min with 2 min final hold time. The injector temperature was maintained at 250°C. Helium was used as a carrier gas at a linear velocity of 39.7 cm/sec and pressure of 68.1 kPa with a flow rate of 1.2 mL/min. One µL of KL juice dissolved in hexane was injected into GC with a split ratio of 1:10. Mass spectrum was obtained in electron ionization mode at 70 eV and the mass spectra were measured in a scan range from 50 to 500 amu. The ion source temperature was 200 °C. Interpretation of compounds was completed by comparing and matching the mass spectra of each compound present in the KL juice with that of standard spectra in the NIST 2005 MS library and the literature (Sparkman 1997). By calculating the average peak area to the total area, the relative percentage of each compound was measured.

Green Synthesis of ZnO Nanoparticles

Green synthesis of ZnO nanoparticles was carried out using a soft chemical method. The precursor material, zinc acetate dihydrate (6.58 g), was taken in a beaker containing 150 mL of deionized water (DW), and 20 mL of filtered raw KL juice was added. This mixture was stirred continuously for 1 h. Sodium hydroxide (NaOH) solution was added drop by drop to this starting solution to maintain the pH at 8.5. The solution was heated up to 80 °C, stirred for 2 h, and cooled to room temperature. After 24 h, by filtration, the settled precipitate was separated and washed with a mixture of ethanol and water in a ratio of 1:3. To get a final product, it was calcinated for 2 h at 400 °C in a muffle furnace.

Characterization Study

The crystalline structure of biosynthesized nanoparticles was analyzed using an X-Ray diffractometer (XRD-PAN analytical-PW 340/60 X′ pert PRO) with Cu-kα radiation (λ=1.5406Å). The optical property of the resultant nanoproducts was determined using UV-Vis-NIR double beam spectrophotometer (LAMBD-35). Fourier-transform infrared (FTIR) spectra were recorded using PerkinElmer RX-I FTIR spectrophotometer. The surface morphology of synthesized nanoparticles was observed using a scanning electron

microscope (SEM-TESCAN VEGA-3) and transmission electron microscope (TEM).

Toxicity Test

Earthworms

The adult earthworms, *E. eugeniae,* were collected from the vermiculture tank maintained at college campus. They were washed with tap water and placed on wet filter paper kept in the petri dishes for 24 h (in the dark at 20 °C) to void the gut contents.

Filter paper contact method

The filter paper contact toxicity method of OECD (Guideline No. 207) (OECD, 1984) was adopted, using 9 cm diameter petri dishes. Different concentrations (0, 100, 200, 300, 400, 500, 600, 700, 800, 900, and 1000 mg/L) of ZnO:KL NPs were suspended in DW and were subjected to sonication for 5 min. Two mL of the suspension was pipetted onto the paper surfaces to moisten the filter paper. Adult earthworms with developed clitellate ranging between 800 to 1000 mg, after voiding the gut content, were used. In the control groups, the earthworms were placed on the filter paper treated with DW only. Each animal was placed individually in a petri dish, and 10 replicates were used for each treatment. After the addition of earthworms, each dish was closed with a plastic lid in which several small ventilation holes were made. All petri dishes were placed in the dark at 25°C. After 48 h of exposure, animal mortality, phenotypic changes, and histology of skin were observed. This experiment was repeated three times (Li *et al.* 2011).

Phenotypic Study

As phenotypic changes in an animal are the first sign of damage to the animal, the phenotypic changes such as color change, coiling, swelling in clitellum, and changes in movement were observed in all the treated groups of earthworms and cumulative data are represented (Samrot *et al.* 2017).

Histological Study

Histological slides of earthworm skin were prepared using the conventional ethyl alcohol dehydration and hematoxylin-eosin staining method. Five earthworms from each treatment group and control were taken and killed using 10% formalin. The skin was dissected using a sterile surgical blade. To avoid tissue damage, the samples were transferred to formalin and kept for 3 h. The tissues were subjected to dehydration through ethanol series to remove water, infiltrated with wax, and entrenched in paraffin. The fixed tissues were sliced using microtome into 1 µm films and subjected to hematoxylin and eosin staining. After staining, all the sections were visualized under a microscope and photographed (Samrot *et al.* 2017).

Absorption, Distribution, Metabolism and Excretion (ADME) Analysis

The pharmacokinetics and drug-likeness of the selected compounds (vitamin C and citric acid) were evaluated using the SwissADME, a free web tool. The Canonical SMILES for the chemical compounds were briefly retrieved from PubChem. The obtained Canonical SMILES were used as input on the SwissADME website. The output files and images were exported directly from the website (Amalraj *et al.* 2023; Murugesan *et al.* 2024; Murugesan and Kaleeswaran 2024).

Molecular Docking

Using the docking software, Molecular Operating Environment (MOE, Ver. 2015.10) based on the standard method (Shah *et al.* 2021), the binding affinity of the selected phytocompounds (ligands) with the target protein molecule, collagen was analyzed. The 3D structures of the selected compounds, vitamin C and citric acid were downloaded from PubChem. To perform docking simulation, the energy-minimized ligands were loaded into MOE. From the Protein Data Bank, the 3D structure of protein molecule, collagen – PDB ID:2F6A was obtained and loaded into MOE. The water molecules and heteroatoms were removed, and polar hydrogens were added. The structure was energy-minimized in the MMFF94x force field to an RMS gradient of 0.05. The energy-minimized conformation of protein was then subjected to 10 ns molecular dynamic simulations at a constant temperature of 300 K, heat time of 10 ps, and temperature relaxation of 0.2 ps.

Statistical Analysis

The test of significance was done using ANOVA with the Tukey comparison test. The P value of < 0.05 was statistically significant. The software, GraphPad Prism(version 9.3), was used for the graphical representation of obtained data.

RESULTS AND DISCUSSION

Preliminary Phytochemical Screening

The phytochemical study of KL juice revealed a broad variety of phytochemicals (Table 1). The primary phytochemical constituents such as alkaloids, phenols, flavonoids, terpenoids, quinones, tannins, and steroids were screened from KL juice. In addition, the ZnO:KL NPs were also subjected to screen the phytochemicals and it showed only the presence of phenols and flavonoids. In previous studies, it was reported that the presence of OH groups in phenols and flavonoids is responsible for the reduction of zinc nitrate into ZnO NPs (Weng *et al.* 2017). Moreover, it was found that phenols and flavonoids are involved in the green synthesis process as a stabilizing and bio-reduction agent for the formation of metal oxide NPs.

Table 1. PreliminaryPhytochemical Analysis

S.No.	Phytochemicals	KL juice*	ZnO:KL NPs*
1.	Alkaloids	+	-
2.	Phenols	+	+
3.	Flavonoids	+	+
4.	Terpenoids	+	-
5.	Quiones	+	-
6.	Tannins	+	-
7.	Steroids	+	-

*KL juice-Kaffir lime juice; ZnO:KL NPs-Kaffir lime fruit juice powered zinc oxide nanoparticles

Quantitative Analysis of Phenols and Flavonoids

Total phenol was estimated using the Folin-Ciocalteu method and Total flavonoids was estimated using the aluminium chloride colorimetric method. The phenols and flavonoids were quantified from the raw juice of kaffir lime and ZnO:KL nanoparticles as only they were screened from the ZnO:KL NPs. As shown in Fig. 1, the total phenols and

flavonoids contents were found to be high in raw juice (77.94±0.26 mg/mL and 62.41±1.44 mg/mL, respectively), and low (58.91±0.15 mg/mL and 46.58±1.44 mg/mL, respectively) in ZnO:KL NPs. Further, when compared, the total phenol content was higher in both samples than the total flavonoid. It has been reported that the presence of OH groups in phenols and flavonoids is responsible for the reduction of zinc nitrate into ZnO NPs (Weng *et al.*, 2017). Phenols and flavonoids in plant materials are used as bio-reductants of metallic ions and display a wide range of biological activities(El-Sawaf et al. 2024). The total phenol and flavonoid contents were quantified from the green ZnO nanoparticles for the first time.

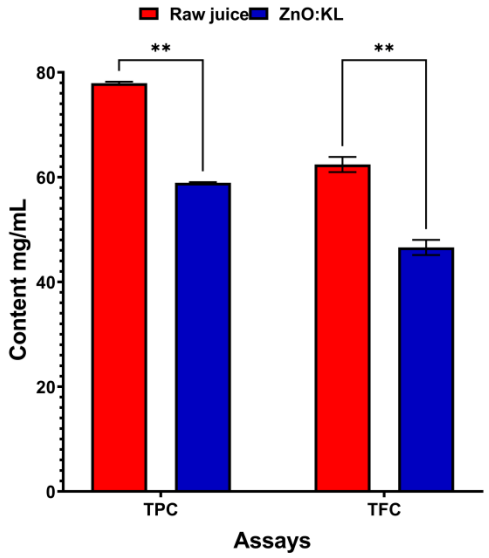

Fig. 1. Total phenolic and flavonoids content of KL juice and ZnO:KL NPs.
* show significant values (***P* ≤0.01)

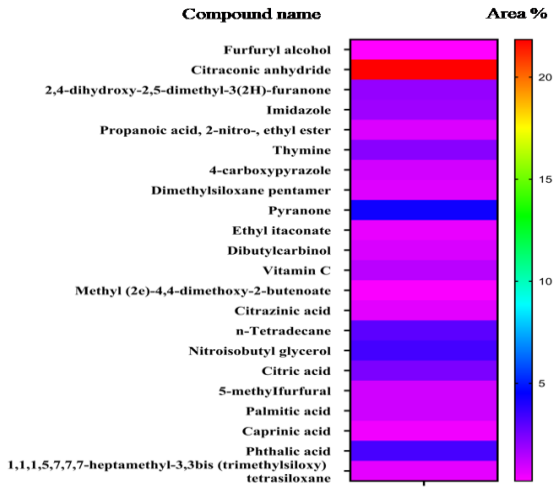

Fig. 2. Heat map of bioactive compounds in the KL juice

GC-MS Analysis of Kl Juice

The GCMS spectrum of KL juice revealed the presence of various bioactive compounds. The bioactive compounds were identified by relating their peak retention time and peak area (%) (Fig. 2). Twenty-two bioactive compounds were identified. Only one

compound, citraconic anhydride (21.84), was a major constituent of the raw juice. Citraconic anhydride is a significant compound as it has a functional group responsible for the capping, stabilizing, and reducing agents during nanoparticle synthesis.

Observation of Color Changes During ZnO NPs Formation

The addition of KL juice to zinc acetate dihydrate solution led to color changes (Fig. 3). The color change observed in the green synthesized ZnO nanoparticles can be primarily linked to the optical properties influenced by the size of the nanoparticles. ZnO:KL NPs, scatter light more effectively than bare ZnO NPs, leading to a more noticeable color change from pale yellow to off-white. This difference in light scattering is influenced by the quantum confinement effect, where bare ZnO NPs have a larger energy band gap, absorbing higher energy light, and thus resulting in different light absorption characteristics. In contrast, ZnO:KL NPs have a smaller band gap, leading to a broader absorption spectrum and increased scattering, which contributes to the more significant color change observed in the green synthesis process(Raza *et al.* 2024). These color changes indicated the formation of ZnO NPs. Naseer *et al*. (2020) observed the color changes during the formation of zinc ions to ZnO NPs and reported that the phytochemical constituents such as phenols and flavonoids are responsible for the formation of NPs.

Fig. 3. Changes in the color of the solution when KL juice was added to zinc acetate dihydrate

Mechanism for Synthesis of ZnO NPs by Using Kaffir Lime Fruit Juice

Based on the reports in the literature and the presence of functional groups in the juice, the possible mechanism for the formation of ZnO NPs is as follows: The hydroxyl groups (OH) and carboxyl (C=O) present in KL juice facilitate the formation of ZnO NPs through the transfer of electrons from hydroxyl groups to the Zn^{2+} ions (Klinbumrung *et al.* 2022). The possible mechanism for the formation of the ZnO NPs is shown in Fig. 4.

Fig. 4. Plausible green synthesis mechanism of ZnO NPs formation using kaffir lime juice

Characterization Of ZnO:KL NPs XRD

The XRD pattern of bare ZnO and KL-powered ZnO nanopowders is shown in Fig. 5. The bare ZnO exhibits a hexagonal wurtzite structure with a (101) peak as a preferential orientation. The second and third prominent peaks are (100) and (002), respectively. The KL-powered ZnO pattern also exhibits the same order of intensity of peaks. However, the intensity of all the peaks increased upon the addition of KL juice in the starting solution. This increase in intensity could be caused by the citric acid in the KL juice. It is reported that the increase in intensity and perfect ZnO wurtzite structure is caused by citric acid (Yang *et al.* 2007). Zabiszak *et al.*, (2018) also observed that citric acid can coordinate metal ions, acting as a bridging spacer. Moreover, two feeble additional peaks are observed at 2θ angles 33.5° and 37.7° that are matched well with (104) and (005) peaks of anhydrous citric acid crystal (Kalaimani *et al*. 2019).

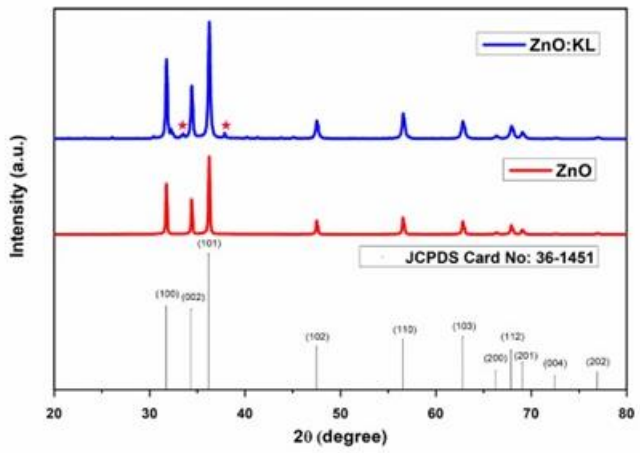

Fig. 5. XRD pattern of bare ZnO and ZnO:KL NPs

UV-Vis-NIR

The UV-Vis-NIR absorption spectra of the prepared ZnO and ZnO:KL are shown in Fig. 6. The absorption edge slightly shifted towards the higher wavelength side, suggesting a slight decrease in the band gap upon KL addition. This decrease in band gap causes the generation of more electron-hole pairs as the material can respond to light of relativity less energy. This generation of more electron-hole pairs generally causes more hydroxyl radicals. These could affect the cell membrane, leading to cell damage. Vitamin

C prevalent in the KL juice acts as a scavenger by donating electrons to the hydroxyl radicals and suppressing their activity on cells. Thus, the addition of KL nullifies the adverse effect of hydroxyl radicals generated in the system and results in a favorable effect.

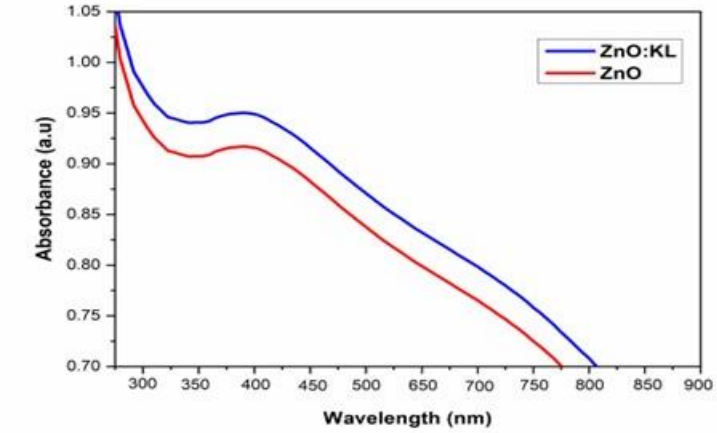

Fig. 6. UV-Vis-NIR spectrum of bare ZnO and ZnO:KL NPs

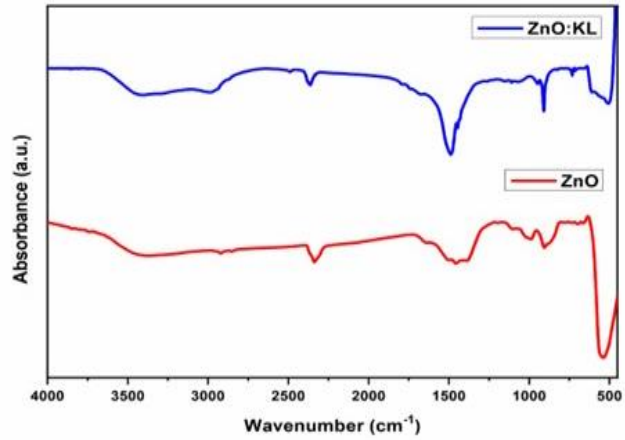

Fig. 7. FTIR spectra of bare ZnO and ZnO:KL NPs

FTIR

The FTIR spectrum of bare ZnO and ZnO:KL NPs is shown in Fig. 7. The peaks in the region of 3500 to 2500 cm^{-1} indicated the presence of characteristic OH (phenols) stretching and bands at 1675 to 1640 cm^{-1} suggested the presence of vitamin C in the system (Bunaciu *et al.* 2009; Othayoth *et al.* 2015). The combined presence of peaks at 1460 to 1410 cm^{-1} indicated the presence of citric acid in the prepared ZnO:KL material (Naseer *et al.* 2020). Spectral peaks at 667 to 500 cm^{-1} and 510 to 698 cm^{-1} confirmed the formation of ZnO nanoparticles (Naseer *et al.* 2020).

Microscopy

The SEM images of bare ZnO and KL powered ZnO are presented in Fig. 8. The bare ZnO had well defined uniform grains with a hexagonal cross section. Upon KL addition, the grains grew with larger cross section but shorter width. However, the hexagonal shape was not affected; the hexagonal cross section is the characteristic feature of ZnO nanomaterials (Ravichandran *et al.* 2022). The better crystalline formation of ZnO:KL seen in SEM images is consistent with the XRD results. (Jiménez-Rosado et al. 2022) reported that polyphenols play a role in preventing nanoparticles aggregation

through their complex structure, provided they retain their antioxidant activity. The experimental results suggest that the growth mechanism of ZnO NPs in hexagonal column form follows the Ostwald ripening mechanism. The key factor affecting ZnO crystal growth are the mass of citric acid and the calcination temperature. Citric acid reduces the solution's surface tension, facilitating crystal formation at lower supersaturation level and forming chelated species with zinc ions, expanding the spatial volume of growth unit. This adsorption of growth units on crystal surfaces influences both speed and orientation of ZnO crystal growth. The larger grain size of the ZnO:KL caused by the citric acid present in the KL juice is favourable for the cell safety of the earthworms. Additionally, OH ions from phenolic compounds affect the growth interface, particularly by modifying the crystal face when OH ions are adsorbed on Zn ions surfaces, promoting nucleation and growth along the C-axis. The larger grain size of the ZnO:KL NPs caused by the citric acid present in the KL juice is favourable for the cell safety of the earthworms. ZnO:KL NPs possess a reduced surface area-to-volume ratio, which slows their dissolution and the release of Zn ions. This results in a reduction in oxidative stress and cellular damage, minimizing the risk of acute toxicity to earthworms. Smaller particles can penetrate the skin and cause severe damage to the cell structure (Deylam *et al.* 2021). The pore diameter of animal skin is in the range of SD 40 nm. Hence, the probability of penetration of ZnO:KL grains(78.0 nm) is less than that of bare ZnO (49.4 nm). The TEM and SADE pattern results support the SEM and XRD results (Fig. 9).

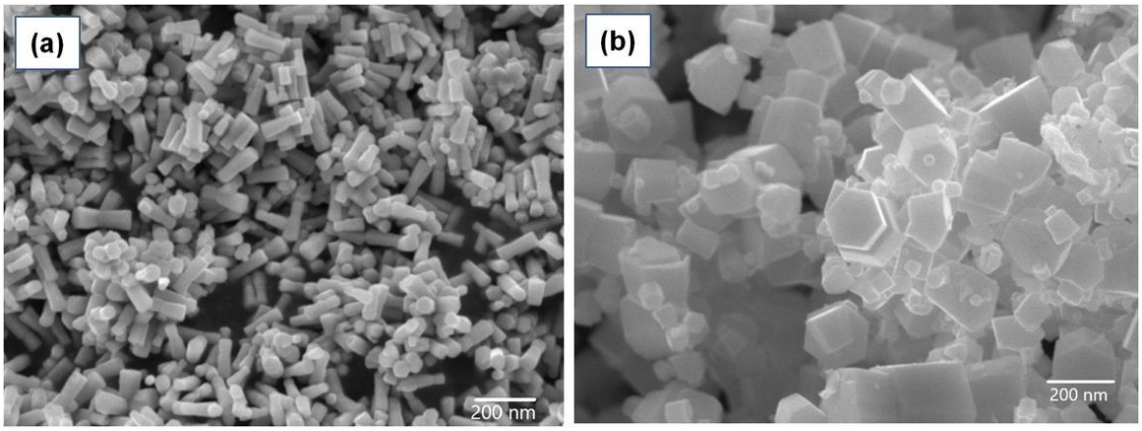

Fig. 8. SEM images: (a) Bare ZnO and (b) ZnO:KL NPs

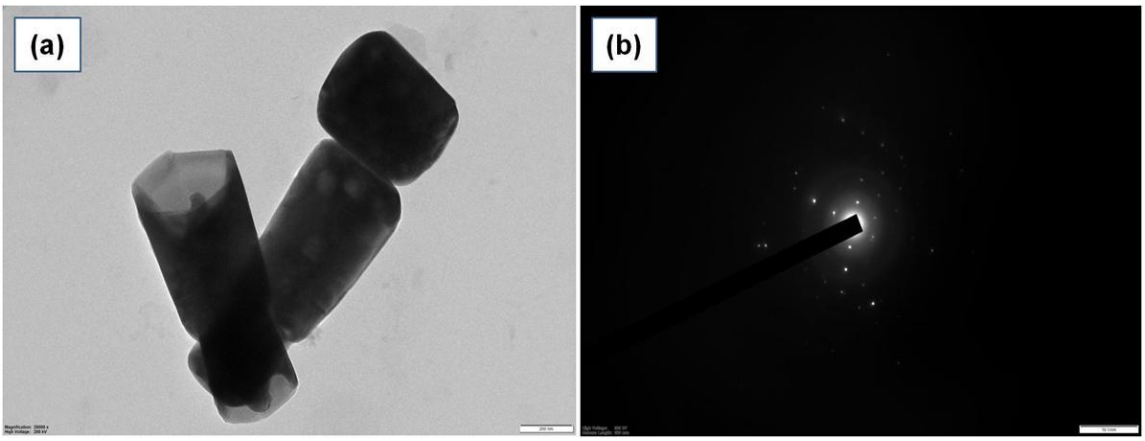

Fig. 9. TEM images of ZnO NPs synthesized using kaffir lime juice with SAED pattern

Phenotypic Changes

The treated earthworms were observed for phenotypic changes, *viz.*, coiling, swelling in clitellum, changes in movement, color change, and mucus secretion, as phenotypic changes of an organism are the first indication of damage to the organism. The results of phenotypic changes observed in all the treated earthworms are presented in Table 2. The earthworms treated with the ZnO:KL NPs did not show any mortality even at tested higher concentrations (1000 mg). However, at the highest tested concentration, earthworms were less active (sluggish movement), and the color of the earthworms changed from the normal purple to brown after 48 h of continuous exposure. The interaction of zinc ions Zn^{2+} with the skin may be the reason for this observed color change in earthworms. The liberated zinc ions could enter the epithelium. Zinc ions are recognized by Troll-like receptors (TLRs) and Pattern Recognition Receptors (PRRs) on the coelomic cells of the earthworm, triggering an immune response. The interaction between nanoparticles and immune receptors activates the Coelomic Cytolytic Factor (CCF). CCF stimulates melanin production as part of the defense mechanism. Melanin helps isolate and neutralize foreign particles. The produced melanin combines with nanoparticles to form brown bodies, resulting in the observed color change on the earthworm's skin. This process of melanization aids in detoxification and production from nanoparticles-induced damage.(Yadav 2015) reported that the melanization process is involved in defense mechanism and also forms brown bodies with nanoparticles. The earthworms treated with 900 mg/L of nanoparticles, earthworms detect stressful conditions, such as zinc ions toxicity or dehydration, using specialized sensory receptors (chemoreceptors) located in the epidermal layer of earthworms detect the zinc ions, triggering a cellular response. These substances are recognized as foreign and potentially damaging to cellular membranes, proteins, and DNA. Chemosensory neurons send electric signals to central nervous system (CNS) *via* nerve fibers along the body wall, where the severity of the stress is assessed. If the stress is deemed harmful, the CNS initiates protective responses, including coiling, behavior. The earthworm contracts its longitudinal and circular muscles, coiling its body to minimize surface contact with harmful substances and reduce water loss. The sensory receptors, maintaining or adjusting its coiled state based on stress level. If conditions improve, the earthworm resume normal activity.

The earthworms treated with 900 and 1000 mg/L nanoparticles exhibited an unusual mucus secretion. Mucus secretion is an adaptive response for the detoxification of ions, as it provides a barrier that protects the epidermis from damage. The mucus is composed of coelomocytes, coelomic fluid, salts, and proteins, which together serve to chelate with Cd (Rodriguez *et al.* 2013). It is reported that mucus secretion is an adaptive response for longer-term detoxification of cadmium (Bouché *et al.* 2000).It is also observed that coelomocytes exposed to Cd may express metallothioneins, which would eliminate Cd from the body.

Sluggish movement in earthworms was observed only in the 1000 mg/L treated group. Earthworm exhibits cutaneous respiration, which depends on the small blood vessels in the body wall. The mucous gland of the epidermis keeps the body wall moisture to ease respiration. When exposed to an increased dose (1000 mg/L) of ZnO:KL, the epidermis and mucous gland could be slightly damaged, which makes it difficult to respire, leading to sluggish movement. Karthikeyan *et al.* (2020) observed sluggish movement in the earthworm *Perionyx excavatus* due to difficulty in respiration when exposed to an increased dose of UV (Subbiahanadar Chelladurai *et al*. 2020).

Table 2. Phenotypic Changes

Treatment (mg)	Colour Change	Coiling	Swelling in Clitellum	Mucus Secretion	Changes in Movement
Control	No	No	No	Usual	No
100	No	No	No	Usual	No
200	No	No	No	Usual	No
300	No	No	No	Usual	No
400	No	No	No	Usual	No
500	No	No	No	Usual	No
600	No	No	No	Usual	No
700	No	No	No	Usual	No
800	No	No	No	Usual	No
900	No	Yes	No	Unusual (Low)	No
1000	Brown	No	No	Unusual (High)	Sluggish

Histological Study

The histological sectioning of the treated earthworms' skin tissue architecture is shown in Fig. 10. No tissue damage was found in the epidermal layer of the skin of earthworms exposed to 100 to 800 mg/L ZnO:KL nanomaterials, whereas the skin of earthworms treated with beyond (900 and 1000 mg/L) the threshold values, were found to have slight tissue damage with collapsed flip structure.

The incorporation of vitamin C and citric acid inherited by kaffir lime fruit extract-powered ZnO nanoparticles with collagen protects the epidermal layer. The skin of earthworms is generally enriched with a protein collagen, which provides structural support to tissues and plays an important role in cellular processes. Goswami *et al.* (2016) reported that collagen can bind with metal ions to form metal chelating. The administration of a lower concentration of Zn resulted in a significant increase in collagen synthesis and supplementation with the higher Zn concentration induced inhibition of collagen synthesis (Andrulewicz-Botulińska *et al.* 2018; Edyta *et al.* 2018). Anonegi *et al.* found that citric acid-incorporated collagen sheets preserved the triple helix structure of the native collagen (Andonegi *et al.* 2020).

Bernstein *et al.* (1977) also found that citric acid increases skin fold thickness in humans. It is reported that vitamin C has important physiological effects on the skin, including the promotion of collagen biosynthesis and acceleration of wound healing (Gref *et al.* 2020).

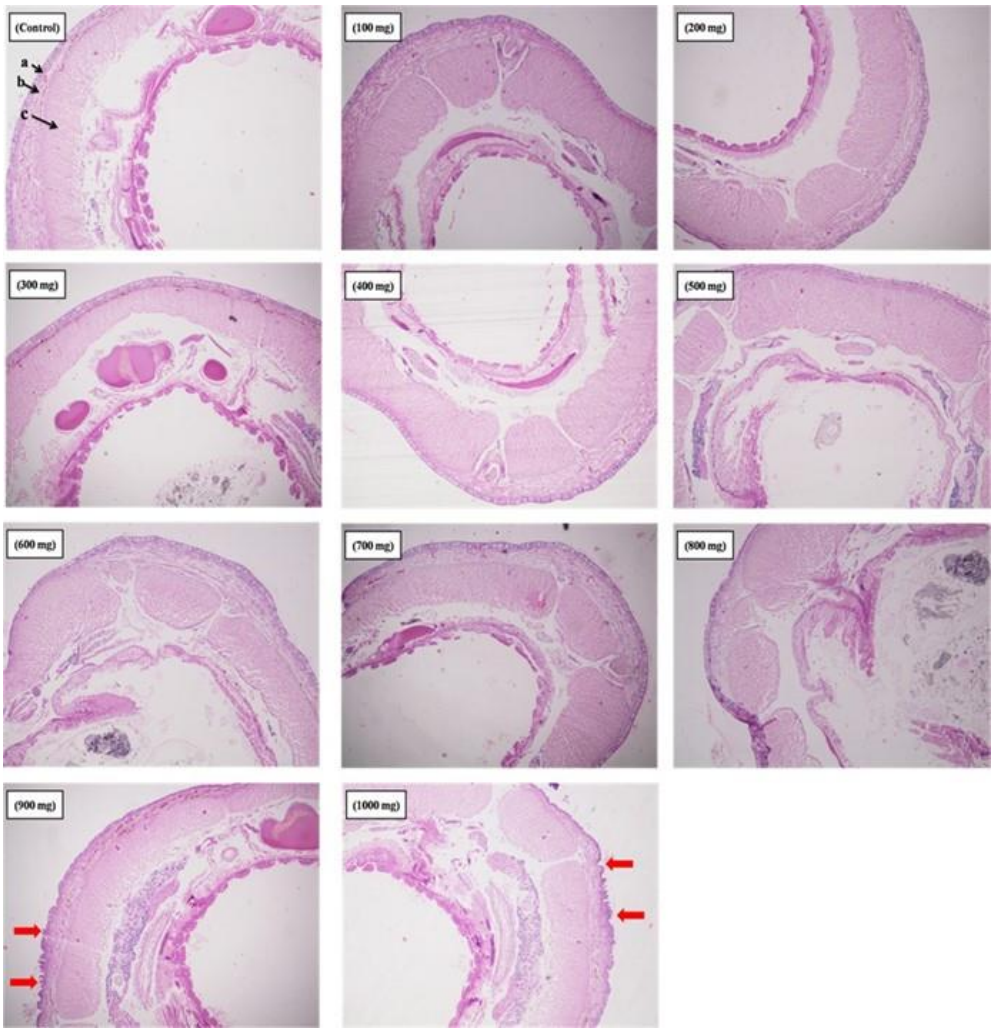

Fig. 10. Histological changes in the skin of tested earthworms, *E. eugeniae* (a - epidermis; b - circular muscle; c-longitudinal muscle, Red arrow indicates skin damage)

In the present observation, the earthworms treated with 900 and 1000 mg/L ZnO:KL NPs demonstrated slight tissue damage in the skin. This may be due to the generation of reactive oxygen species because of the high accumulation of Zn^{2+} ions in the epidermal layer. Due to the water supply, hydrolysis occurs in the stratum corneum, the first layer of the epidermis, which results in the liberation and accumulation of Zn^{2+} ions in the epidermal layer. The accumulation of Zn^{2+} ions is higher if the concentration of applied ZnO:KL nanoparticles is higher. The Zn^{2+} ions, thus formed generate reactive oxygen species which cause tissue damage. The hypothetical description is illustrated in Fig. 11.

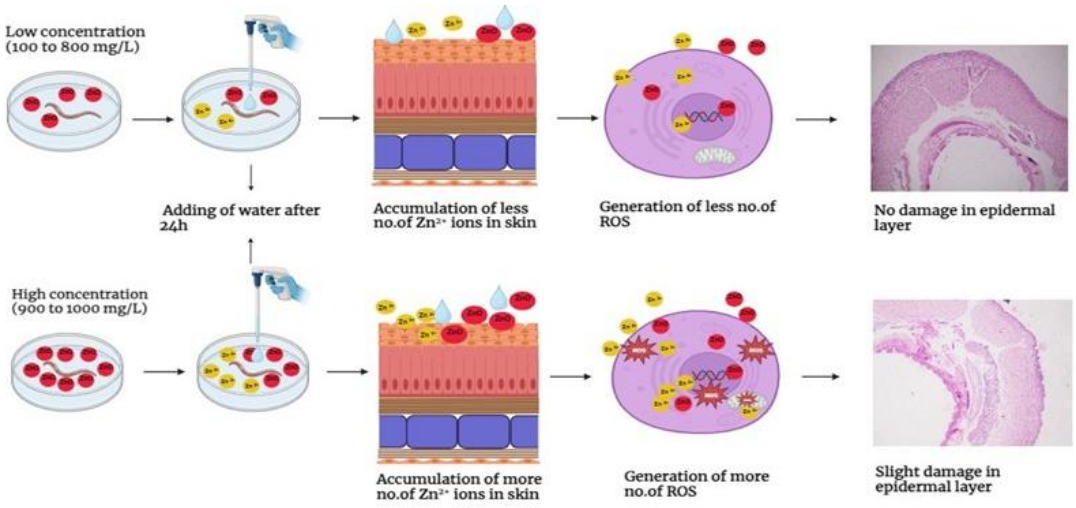

Fig.11. Schematic diagram showing the proposed biphasic effect mechanism of the ZnO:KL NPs

Molecular Docking

The selected bioactive compounds such as vitamin C and citric acid predominantly identified in GC-MS analysis were subjected to molecular docking to reveal their binding affinity with the protein, collagen. These compounds were selected based on Lipinski's rule (Table 3).

Table 3. ADME Analysis of Selected Bioactive Compounds

Molecule	Citric acid	Vitamin C
Molecular formula	C6H8O7	C6H8O6
Molecular weight	192.12	176.12
Number of H-bond acceptors	7	6
Number of H-bond donors	4	4
Log P (<5)*	1.49	0.31
TPSA (<140)*	132.13	107.22
Lipinski violations count	0	0
*TPSA- Topological surface area, Log P- Lipophilicity		

The selected compounds were docked to the receptor protein using the MOE software, and the results are given in Table 4. It was found that vitamin C can bind to the collagen protein in a favorable orientation and achieve a binding affinity of -4.44 kcal/mol. Figure 12a shows the interaction of vitamin C with three amino acid residues, *viz.*, Arg17, Gly16, and Thr18 of collagen through hydrogen-hydrogen bonding.

Table 4. Binding Affinities and Potential Molecular Interactions of Vitamin C and Citric Acid with Collagen

Compound	Docking Score (kcal/mole)	RMSD (Å)	Type of Interactions	Bond Length (Å)	Amino acid Residues
Citric acid	-4.97	1.71	H-H	3.34	Ans 225
			H-H	2.96	Ser 274
			H-H	3.1	Thr 227
Vitamin C	-4.44	1.33	H-H	2.91	Arg 17
			H-H	2.97	Gly 16
			H-H	3.13	Thr 18

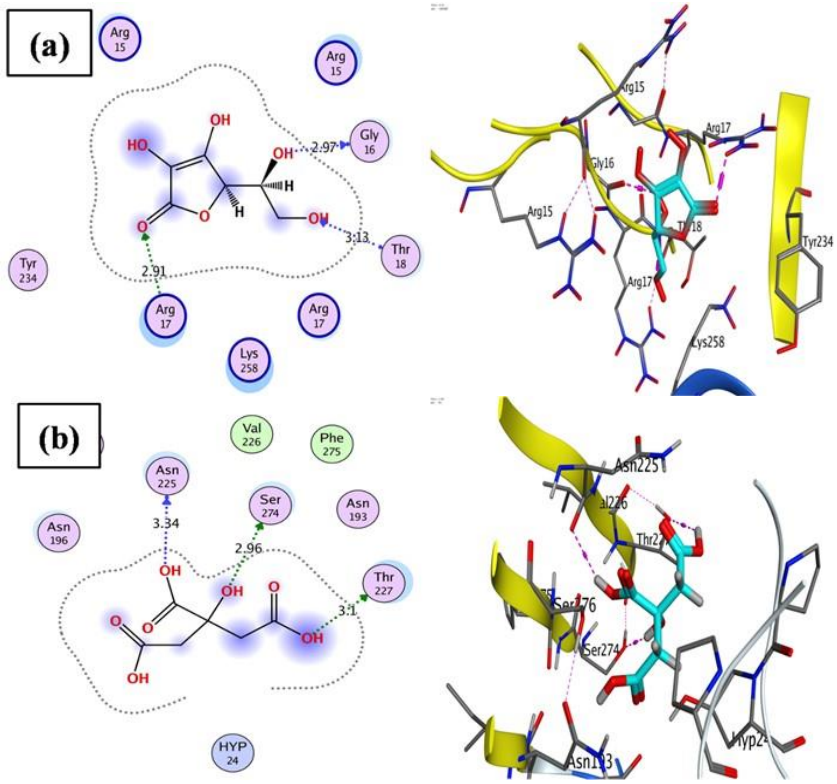

Fig. 12. Binding of selected bioactive compounds, vitamin C (a) and citric acid (b) with collagen

This interaction suggests that vitamin C can form a stable and long-term bond with the collagen protein. Gref *et al.* (2020) reported that vitamin C has an important physiologic effect on the skin of humans including promotion of collagen biosynthesis and acceleration of wound healing. Boyce *et al.* (2002) reported that vitamin C improves the anatomy and physiology of cultured skin and promotes cellular viability and formation of the epidermal barrier *in vitro*.

The collagen of earthworms is similar to that of vertebrates (Vavoulidou *et al.* 2010). In the present study, citric acid was bound to the collagen in a favorable orientation and achieved a binding affinity of -4.97 kcal/mol. The favorable orientation of citric acid with Asn225, Ser274, and Thr227 amino acid residues of collagen is shown in Fig. 12b. This result indicates that citric acid binds to collagen with high affinity and forms a stable complex. In a previous study, it was reported that citric acid plays a crucial role in increasing skinfold thickness. Ruey *et al.* (2004) reported that citric acid stimulates the biosynthesis of collagen fibers (Yu and Van Scott 2004). From the molecular docking of the present study, it was confirmed that vitamin C and citric acid have the potential to interact with the collagen protein. As vitamin C and citric acid influence the biosynthesis of collagen, they could be promising candidates to prevent the skin damage caused by liberated Zn^{2+} ions from the kaffir lime-activated ZnO nanoparticles.

CONCLUSIONS

Green ZnO nanoparticles synthesized using kaffir lime fruit juice exhibited less toxicity to earthworm, *E. eugeniae*. As per the earlier reports, chemically synthesized ZnO nanoparticles cause mortality at 500 mg/L. But in the present study, the earthworms exposed to green ZnO nanoparticles led its normal life upto 800 mg/L, and interestingly no mortality was found even at 1000 mg/L. From the results, it is understood that the phytochemicals present in the kaffir lime fruit juice make the ZnO nanoparticles more biocompatible and eco-friendly. Hence, it is concluded that the usage of chemically synthesized ZnO nanoparticles in various fields could be replaced by the green ZnO nanoparticles to minimize the environmental hazards of nano pollution.

ACKNOWLEDGMENTS

The authors extend their appreciation to the Researchers supporting project number (RSP2024R11) at King Saud University, Riyadh, Saudi Arabia. The authors are grateful to PG & Research Department of Zoology for providing the necessary facilities and the authors are very thankful to Dr. K. Ravichandran, Associate Professor & Head, PG & Research Department of Zoology, A.V.V.M. Sri Pushpam College (Autonomous), Poondi, Thanjavur district, Tamil Nadu, India for his timely suggestion and technical support.

Credit Author Statement

Sampath Paventhan: Investigation, Data Curation, Writing-original Draft, Visualization; Pazhanisamy Kavitha: Conceptualization, Methodology, Writing-original Draft, Visualization, Supervision; Balasubramanian Kaleeswaran: Resource, Investigation, Data Curation; Muniappan Ayyanar: Methodology, Investigation, Resource; Vengamuthu Subramanian Kavitha; Raman Sripriya: Visualization, Methodology, Data Curation; Singamoorthy Amalraj: Writing-original Draft, Resource, Visualization; R. Rajakrishnan: Investigation, Resource; Ahmed Alfarhan: Resource, Investigation.

REFERENCES CITED

Amalraj, S., Gurav, S.S., Kalaskar, M.G., Maroyi, A., and Ayyanar, M. (2023). "Hypoglycemic, anti-inflammatory, and anti-aging potential of *Canthium coromandelicum* (Burm.f.) Alston leaf extracts: *In vitro* and *in silico* ADMET studies," *South African J. Bot.* 161, 377-387. DOI: 10.1016/j.sajb.2023.08.036

Amalraj, S., Mariyammal, V., Murugan, R., Gurav, S.S., Krupa, J., and Ayyanar, M. (2021). "Comparative evaluation on chemical composition, in vitro antioxidant, antidiabetic and antibacterial activities of various solvent extracts of *Dregea volubilis* leaves," *South African J. Bot.* 138, 115-123. DOI: 10.1016/j.sajb.2020.12.013

Andonegi, M., de la Caba, K., and Guerrero, P. (2020). "Effect of citric acid on collagen sheets processed by compression," *Food Hydrocoll.* 100, article 105427. DOI: 10.1016/j.foodhyd.2019.105427

Andrulewicz-Botulińska, E., Wiśniewska, R., Brzóska, M.M., Rogalska, J., and Galicka, A. (2018). "Beneficial impact of zinc supplementation on the collagen in the bone

tissue of cadmium-exposed rats," *J. Appl. Toxicol*. 38, 996-1007. DOI: 10.1002/jat.3608

Bouché, M.L., Habets, F., Biagianti-Risbourg, S., and Vernet, G. (2000). "Toxic effects and bioaccumulation of cadmium in the aquatic oligochaete *Tubifex tubifex*," *Ecotoxicol. Environ. Saf.* 46, 246-251. DOI: 10.1006/eesa.2000.1919

Boyce, S.T., Supp, A.P., Swope, V.B., and Warden, G.D. (2002). "Vitamin C regulates keratinocyte viability, epidermal barrier, and basement membrane *in vitro*, and reduces wound contraction after grafting of cultured skin substitutes," *J. Invest. Dermatol.* 118, 565-572. DOI: 10.1046/j.1523-1747.2002.01717.x

Bunaciu, A.A., Bacalum, E., Aboul-Enein, H.Y., Udristioiu, G.E., and Fleschin, Ş. (2009). "FT-IR spectrophotometric analysis of ascorbic acid and biotin and their pharmaceutical formulations," *Anal. Lett*. 42, 1321-1327. DOI: 10.1080/00032710902954490

Daimari, J., and Deka, A.K. (2024). "Anticancer, antimicrobial and antioxidant activity of CuO–ZnO bimetallic nanoparticles: Green synthesised from *Eryngium foetidum* leaf extract," *Sci. Rep.* 14, 1-14. DOI: 10.1038/s41598-024-69847-w

Deylam, M., Alizadeh, E., Sarikhani, M., Hejazy, M., and Firouzamandi, M. (2021). "Zinc oxide nanoparticles promote the aging process in a size-dependent manner," *J. Mater. Sci. Mater. Med*. 32. DOI: 10.1007/s10856-021-06602-x

El-Sawaf, A.K., El-Moslamy, S.H., Kamoun, E.A., and Hossain, K. (2024). "Green synthesis of trimetallic CuO/Ag/ZnO nanocomposite using *Ziziphus spina*-christi plant extract: Characterization, statistically experimental designs, and antimicrobial assessment," *Sci. Rep*. 14, 1-24. DOI: 10.1038/s41598-024-67579-5

Filipiak, Z.M., and Bednarska, A.J. (2021). "Different effects of Zn nanoparticles and ions on growth and cellular respiration in the earthworm *Eisenia andrei* after long-term exposure," *Ecotoxicology* 30, 459-469. DOI: 10.1007/s10646-021-02360-2

Goswami, L., Pratihar, S., Dasgupta, S., Bhattacharyya, P., Mudoi, P., Bora, J., Bhattacharya, S.S., and Kim, K.H. (2016). "Exploring metal detoxification and accumulation potential during vermicomposting of tea factory coal ash: Sequential extraction and fluorescence probe analysis," *Sci. Rep.* 6, 1-13. DOI: 10.1038/srep30402

Gref, R., Deloménie, C., Maksimenko, A., Gouadon, E., Percoco, G., Lati, E., Desmaële, D., Zouhiri, F.,and Couvreur, P. (2020). "Vitamin C–squalene bioconjugate promotes epidermal thickening and collagen production in human skin," *Sci. Rep*. 10, 1-12. DOI: 10.1038/s41598-020-72704-1

Harborne, J. B. (1998). *Phytochemical Methods. A Guide to Modern Techniques of Plant Analysis*, 5th Edition, Chapman and Hall Ltd, London,Springer Dordrecht.

Jiménez-Rosado, M., Gomez-Zavaglia, A., Guerrero, A., andRomero, A. (2022). "Green synthesis of ZnO nanoparticles using polyphenol extracts from pepper waste (*Capsicum annuum*)," *J. Clean. Prod*. 350. DOI: 10.1016/j.jclepro.2022.131541

Kalaimani, N., Ramya, K,. Vinitha, G,. Aarthi, R,. Ramachandra Raja. C. (2019). "Structural, spectral, thermal and nonlinear optical analysis of anhydrous citric acid crystal," *Optik* (Stuttg). 192, article 162960. DOI: 10.1016/j.ijleo.2019.162960

Klinbumrung, A., Panya, R., Pung-Ngama, A., Nasomjai, P., Saowalakmeka, J., and Sirirak, R. (2022). "Green synthesis of ZnO nanoparticles by pineapple peel extract from various alkali sources," *J. Asian Ceram. Soc*. 10, 755-765. DOI: 10.1080/21870764.2022.2127504

Li, L.Z., Zhou, D.M., Peijnenburg, W.J.G.M., van Gestel, C.A.M., Jin, S.Y., Wang, Y.J.,

and Wang, P. (2011). "Toxicity of zinc oxide nanoparticles in the earthworm, *Eisenia fetida* and subcellular fractionation of Zn," *Environ. Int*. 37, 1098-1104. DOI: 10.1016/j.envint.2011.01.008

Li, M., Yang, Y., Xie, J., Xu, G., and Yu, Y. (2019). "*In-vivo* and *in-vitro* tests to assess toxic mechanisms of nano ZnO to earthworms," *Sci. Total Environ*. 687, 71-76. DOI: 10.1016/j.scitotenv.2019.05.476

Murugesan, M., and Kaleeswaran, B. (2024). "*In silico* drug discovery: Unveiling potential targets in *Plasmodium falciparum*," *AspectsMolecul. Med.*3, 100038. DOI:10.1016/j.amolm.2024.100038

Murugesan, R., Vasuki, K., and Kaleeswaran, B. (2024). "A green alternative: Evaluation of *Solanum torvum* (Sw.) leaf extract for control of *Aedes aegypti* (L.) and its molecular docking potential," *Intelligent Pharmacy*, 2(2), 251–262. DOI: 10.1016/j.ipha.2023.11.012

Naseer, M., Aslam, U., Khalid, B., and Chen, B. (2020). "Green route to synthesize zinc oxide nanoparticles using leaf extracts of *Cassia fistula* and *Melia azadarach* and their antibacterial potential," *Sci. Rep.* 10, 1-10. DOI: 10.1038/s41598-020-65949-3

OECD (1984). "Earthworm, acute toxicity tests," *OECD Guidel. Test. Chem.* 1, 1–9.

Othayoth, R., Mathi, P., Bheemanapally, K., Kakarla, L., and Botlagunta, M. (2015). "Characterization of vitamin-cisplatin-loaded chitosan nano-particles for chemoprevention and cancer fatigue," *J. Microencapsul*. 32, 578-588. DOI: 10.3109/02652048.2015.1065921

Ravichandran, K., Vasanthi, D.S., Kavitha, P., Shalini, R., Suvathi, S., and Praseetha, P.K. (2022). "Cost-effective and eco-friendly dye degradation by enzyme-powered ZnO nanomaterial: Effect of process temperature," *Bull. Mater. Sci.* 45. DOI: 10.1007/s12034-021-02619-8

Raza, A., Malan, P., Ahmad, I., Khan, A., Haris, M., Zahid, Z., Jameel, M., Ahmad, A., Seth, C. S., Asseri, T. A. Y., Hashem, M., and Ahmad, F. (2024). "*Polyalthia longifolia*-mediated green synthesis of zinc oxide nanoparticles: characterization, photocatalytic and antifungal activities," *RSC Adv*, 14(25), 17535–17546. DOI: 10.1039/d4ra01035c

Rodriguez, M. G., Rivera, B. H., Ventura-Juárez, J., and Muñoz-Ortega, M. H. (2013). "Cadmium toxicity evaluation in the earthworm *Eisenia foetida*: Behavior and histopathological effects," *Trends Comp. Biochem. Physiol.* 17, 81-92.

Samrot, A. V., Justin, C., Padmanaban, S., and Burman, U. (2017). "A study on the effect of chemically synthesized magnetite nanoparticles on earthworm: *Eudrilus eugeniae*," *Appl. Nanosci.* 7, 17-23. DOI: 10.1007/s13204-016-0542-y

Selvaraj, R., Pai, S., Murugesan, G., Pandey, S., Bhole, R., Gonsalves, D., Varadavenkatesan, T., and Vinayagam, R. (2021). "Green synthesis of magnetic α–Fe_2O_3 nanospheres using *Bridelia retusa* leaf extract for Fenton-like degradation of crystal violet dye,"*Appl. Nanosci*. 11, 2227-2234. DOI:10.1007/s13204-021-01952-y

Shah, M., Murad, W., Rehman, N.U., Mubin, S., Al-Sabahi, J.N., Ahmad, M., Zahoor, M., Ullah, O., Waqas, M., Ullah, S., Kamal, Z., Almeer, R., Bungau, S.G., and Al-Harrasi, A. (2021). "GC-MS analysis and biomedical therapy of oil from n-hexane fraction of *Scutellaria edelbergii* Rech. F.: *In vitro*, *in vivo*, and *in silico* approach," *Molecules* 26. DOI: 10.3390/molecules26247676

Sparkman, O.D. (1997). "Identification of essential oil components by gas chromatography / mass spectroscopy," *J. Am. Soc. Mass Spectrom*. 8, 671-672. DOI: 10.1016/s1044-0305(97)00026-3

Subbiahanadar Chelladurai, K., Selvan Christyraj, J.D., Azhagesan, A., Paulraj, V.D., Jothimani, M., Yesudhason, B.V., Chellathurai Vasantha, N., Ganesan, M., Rajagopalan, K., Venkatachalam, S., Benedict, J., John Samuel, J.K., and Selvan Christyraj, J.R.S. (2020). "Exploring the effect of UV-C radiation on earthworm and understanding its genomic integrity in the context of H2AX expression," *Sci. Rep*. 10, 1-14. DOI: 10.1038/s41598-020-77719-2

Świątek, Z.M., Woźnicka, O., and Bednarska, A.J. (2020). "Unravelling the ZnO-NPs mechanistic pathway: Cellular changes and altered morphology in the gastrointestinal tract of the earthworm *Eisenia andrei*," *Ecotoxicol. Environ. Saf*. 196, article 110532. DOI: 10.1016/j.ecoenv.2020.110532

Valerio-Rodríguez, M.F., Trejo-Téllez, L.I., Aguilar-González, M.Á., Medina-Pérez, G., Zúñiga-Enríquez, J.C., Ortegón-Pérez, A., and Fernández-Luqueño, F. (2020). "Effects of ZnO, TiO_2 or Fe_2O_3 nanoparticles on the body mass, reproduction, and survival of *Eisenia fetida*," *Polish J. Environ. Stud*. 29, 2383-2394. DOI: 10.15244/pjoes/100668

Vavoulidou, E., Dellaporta, L., and Bilalis, D.J. (2010). "Collagen distribution in the tissue of the earthworm *Octodrilus complanatus*: (Oligochaeta: Lumbricidae)," *Zool. Middle East* 51, 175-180. DOI: 10.1080/09397140.2010.10638471

Weng, X., Guo, M., Luo, F., and Chen, Z. (2017). "One-step green synthesis of bimetallic Fe/Ni nanoparticles by eucalyptus leaf extract: Biomolecules identification, characterization and catalytic activity," *Chem. Eng. J.* 308, 904-911. DOI: 10.1016/j.cej.2016.09.134

Yadav, S. (2015). "Presence of Au-NPs in coelomic cells of earthworm *Eudichogaster prashadi* Stephenson," *Int. J. Curr. Microbiol. Appl. Sci*. 4, 1013–1021.

Yang, Z., Liu, Q.H., and Yang, L. (2007). "The effects of addition of citric acid on the morphologies of ZnO nanorods," *Mater. Res. Bull.* 42, 221-227. DOI: 10.1016/j.materresbull.2006.06.009

Yu, R.J., and Van Scott, E.J. (2004). "Alpha-hydroxyacids and carboxylic acids," *J. Cosmet. Dermatol.* 3, 76-87. DOI: 10.1111/j.1473-2130.2004.00059.x

Zabiszak, M., Nowak, M., Taras-Goslinska, K., Kaczmarek, M.T., Hnatejko, Z., and Jastrzab, R. (2018). "Carboxyl groups of citric acid in the process of complex formation with bivalent and trivalent metal ions in biological systems," *J. Inorg. Biochem.* 182, 37-47. DOI: 10.1016/j.jinorgbio.2018.01.017

Article submitted: July 3, 2024; Peer review completed: August 24, 2024; Revised version received: November 17, 2024; Further revisions received and accepted: November 24, 2024; Published: December 11, 2024.
DOI: 10.15376/biores.20.1.1345-1364